Available online at www.sciencedirect.com
ScienceDirect
Journal of Photochemistry and Photobiology A: Chemistry 186 (2007) 194–201
Journal of Photochemistry and Photobiology A:Chemistry
www.elsevier.com/locate/jphotochem

Study on the multirecognition mechanism of supramolecular interaction in the thiabendazole/β-cyclodextrin/Triton X-100

Xu Wang, Jing Wang, Yan Wang, Zhen Zhen Chen, Bo Tang *

College of Chemistry, Chemical Engineering and Materials Science, Shandong Normal University, Jinan 250014, China

Received 25 December 2005; received in revised form 30 July 2006; accepted 12 August 2006
Available online 22 August 2006

Abstract

A strong and reproducible room temperature phosphorescence (RTP) signal ($\lambda_{ex}/\lambda_{em}$ = 298/481 nm) coming from a 1:1:1 β-cyclodextrin (β-CD)/thiabendazole (TBZ)/Triton X-100 (TX-100) supramolecular ternary inclusion complex was induced by KI, which act as a heavy-atom perturber without removing dissolved oxygen from solution. The multirecognition mechanism of the β-cyclodextrin (β-CD)/thiabendazole (TBZ)/Triton X-100 (TX-100) supramolecular ternary inclusion was studied and discussed by means of phosphorescence spectrum, surface tension of the solution, infra-red spectrograms and ^{1}H NMR spectroscopy. Results showed that the phenyl ring of TBZ and the hydrophobic hydrocarbon chain of TX-100 could enter the hydrophobic cavity of the β-CD to form supramolecular ternary inclusion, which provided an effective protection for RTP of TBZ. Compared with the method using chemical oxygen scavenger, the heavy-atom concentration of the proposed method was decreased about four times, the lifetime of the phosphorescence was prolonged nine times, and the pH range of the supramoleculer interaction was greatly broadened.

Keywords: Thiabendazole; β-Cyclodextrin; TX-100; Ternary inclusion complex; Supramolecular multirecognition; Heavy-atom induced room-temperature phosphorescence

1. Introduction

Cyclodextrins (CDs) (Scheme 1), the cyclic oligosaccharides consisting of six or more D-(+)-glucopyranose units, are well known to accommodate various guest molecules into their truncated cone-shaped hydrophobic cavity in aqueous solution [1–3]. This fascinating property enables them to be successfully used as drug catalyzer [4,5], separation reagents [6], enzyme mimics [7], photochemical sensors [8,9], and catalysis [10], and be used in host–guest interactions [11] and molecular recognitions [12]. Surfactants can provide a similar microenvironment and function like the CDs [13]. Recently, the interactions of surfactants with CDs have attracted much attention since some chemical and physical properties of surfactants can be changed when they are included in CDs cavity [14]. Studies on the formation of multirecognition ternary CDs complexes, in which two different guests are complexed in a single CD host cavity, have been performed [15]. In a drug:CD:surfactant multirecognition ternary complex, drug molecules can show remarkably different spectral characteristics from those to in a binary drug:CD complex, which leads to very high sensitivity and selectivity of the analytical method. It is well accepted that this method has very important theoretical and applicative value.

Thiabendazole [2-(4-thiazolyl)-1H-benzimidazole, TBZ] is formulated as Scheme 2.

Recently, Blanco et al. reported the room temperature phosphorescence (RTP) spectral parameters of some polycyclic aromatic hydrocarbons and nitrogen heterocycles, including TBZ, in aqueous solution without any protective medium [16]. This new type of RTP emission was named as non-protective fluid RTP [17] (NP-RTP) or heavy-atom induced RTP [18] (HAI-RTP). But in that report, the optimization of the chemical variables for the RTP of TBZ was not satisfactory, e.g. the concentration of KI, the heave atom perturbed, was as high as 0.8 mol/L; the phosphorescence lifetime of TBZ was only 89 μs; the pH range was limited to 6.5–10 because of the addition of sodium sulfite as a chemical deoxygenator. So the sensitivity of method is low and the experimental conditions are difficult

* Corresponding author. Tel.: +86 531 6180010; fax: +86 531 6180017.
E-mail address: tangb@sdnu.edu.cn (B. Tang).

1010-6030/$ – see front matter © 2006 Elsevier B.V. All rights reserved.
doi:10.1016/j.jphotochem.2006.08.004

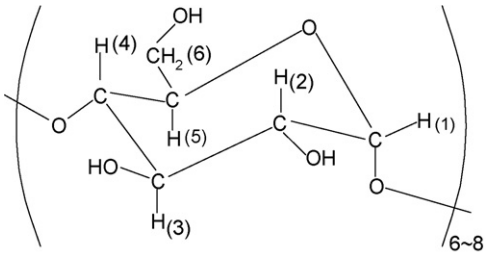

Scheme 1. The structure of CD oligosaccharide.

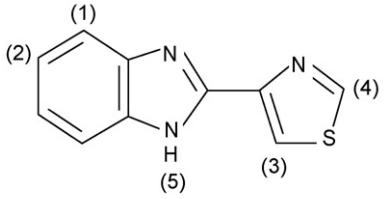

Scheme 2. The chemical structure of TBZ.

to control. In the present work, intense and reproducible RTP from a TBZ/TX-100/β-CD ternary inclusion complex with the stoichiometry of 1:1:1 was observed by using KI as the heavy-atom perturber. Based on the reaction, a novel RTP method of TBZ was established. Compared with the reported HAI-RTP or NP-RTP method, the proposed method need not use chemical oxygen scavenger; the heavy-atom concentration was decreased about four times; the lifetime of the phosphorescence was prolonged nine times; the pH range was greatly broadened.

The mechanism of the supramolecular multirecognition interaction was studied and discussed by means of phosphorescence spectrum, surface tension of the solution, infra-red spectrograms and ^{1}H NMR spectroscopy. The apparent formation constant of the ternary inclusion complex was determined to be 3.42×10^6 L^2/mol^2.

2. Experimental

2.1. Instruments and chemicals

All steady-state luminescence spectra were carried out on a Perkin-Elmer (Norwalk, CT, USA) LS-5 luminometer, equipped with a xenon lamp, 1.0 cm quartz cells and a Perkin-Elmer Model 561 recorder, phosphorescent mode, the delay time (t_d) and gate time (t_g) are 0.15 and 0.25 ms, respectively, and the slit width for excitation and emission are 15 and 20 nm, respectively. Infra-red spectra were obtained from a PE-983G IR-spectrophotometer (Perkin-Elmer). ^{1}H NMR spectra data were recorded at a Varian Inova-300 nuclear magnetic resonance spectrometer (Vrian, Solvent: DMSO-d_6, internal standard: TMS). pH measurements were made with a pHS-3C digital pH-meter (Shanghai Lei Ci Device Works, Shanghai, China). The sample chamber accommodated a thermostated cuvette holder, controlled to 25 ± 1 °C via a CS-50 constant temperature circulator. Surface tension measurements were made using ST-1 surface tensiometer (Shimadzu).

TBZ was of analytical reagent grade. Its stock solution (2.0×10^{-5} g/mL) was prepared in acetonitrile and stored in the dark in amber bottles at 4 °C, diluted to 1.0×10^{-6} g/mL when used. β-CD was purified by twice recrystallization in double-distilled water, followed by vacuum drying at 60 °C for 12 h and used with a concentration of 5.00×10^{-3} mol/L aqueous solution. TX-100 (Fluka) was of analytical reagent and was used in a concentration of 3.0×10^{-3} mol/L aqueous solutions. KI was analytically pure and used with a concentration of 2.00 mol/L aqueous solution. A 0.10 mol/L of sodium citrate–sodium hydroxide buffer solution was used to adjust the solution pH to 5.50. Other chemicals used were of analytical reagent or higher grade. Doubly distilled water was used throughout.

2.2. Synthesis of β-CD–TBZ inclusion complex

According to the reaction routine reported in the reference [19], 0.01 mol TBZ was dissolved in a minimum volume of ethanol at 60 °C and then added dropwise into the 1.5 equiv. of β-CD aqueous solution at 60 °C upon continuous intensive stirring. The mixture solution was refluxed with vigorous agitation at 70 °C for about 4 h, then ethanol was removed at 80–82 °C. After the mixture was cooled to room temperature, it was stirred for 8 h at ambient temperature. The reaction mixture was allow to store overnight at 4 °C, then centrifugalized and filtered on a sintered glass filter. The product was obtained and washed sequentially with doubly distilled water and ethanol, then dried in a vacuum oven at an elevated temperature (60–65 °C). About 7.32 g white crystalline was obtained in 60% yield. m.p.: 268–270 °C, $[\alpha]_D^{25}$: −117.02 °C mL dm^{-1} g^{-1} (determined in methanol/water (1:2) at 25 °C), R_f: 0.47 (GF254 silica gel plates, spread with acetic ether/dichloromethane (1:1) and iodine vapor visualization).

2.3. Experimental procedure

Into a 10 mL colorimetric tube, following solution were added sequentially: 2.00 mL of sodium citrate–sodium hydroxide buffer solution, an aliquot of TBZ stock solution containing 0.0–9.0×10^{-3} mg of TBZ, 1.00 mL of 5.0×10^{-3} mol/L β-CD, 2.00 mL of 3.0×10^{-3} mol/L TX-100 and 1.00 mL of 2 mol/L KI. The mixed solution was diluted to 10 mL with doubly distilled water and allowed to equilibrate at 20 ± 1 °C for 10 min. Then the phosphorescence intensity was measured at $\lambda_{ex}/\lambda_{em}$ = 298/481 nm with t_d/t_g = 0.15/0.25 ms against a reagent blank. This procedure was replicated in order to obtain three or more phosphorescence intensity values for each of the TBZ concentration studied.

Surface tension measurements were made using the hanging slice method [20] at 25 ± 1 °C. About 30–40 measurements were made for a particular solution and the standard deviation of surface tension from the mean value was found to be less than ±0.2 mN m^{-1}.

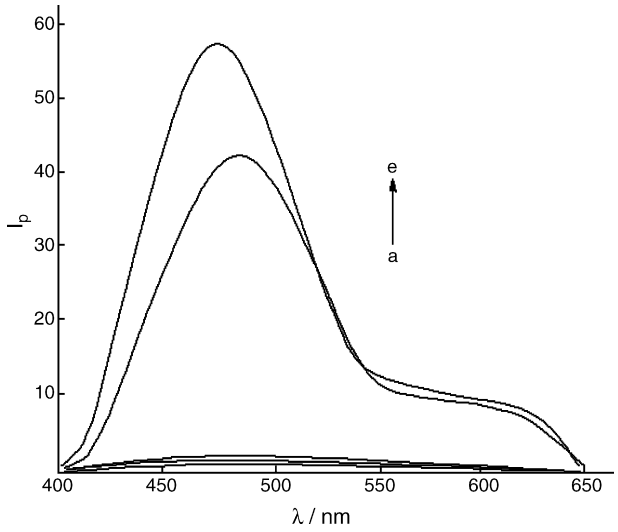

Fig. 1. The room temperature phosphorescence (RTP) spectrum of TBZ: (a) β-CD + TBZ + KI, (b) TX-100 + TBZ + KI, (c) β-CD + TBZ + TX-100, (d) TBZ + Na_2SO_3 + KI [16] and (e) β-CD + TBZ + TX-100 + KI. (a)–(e): *C*(TBZ) 200 μg/L; *C*(β-CD) 5.0×10^{-4} mol/L; *C*(TX-100) 6.0×10^{-4} mol/L; *C*(KI) 0.20 mol/L; pH 5.50; (d) [16]: C(TBZ) 200 μg/L; *C*(Na_2SO_3) 0.001 mol/L; *C*(KI) 0.80 mol/L; pH 6.50.

3. Results and discussion

3.1. RTP spectra

Fig. 1 showed the phosphorescence spectra of TBZ in different media. As could be seen, only in the presence of β-CD or TX-100, phosphorescence was not observed obviously, which indicated that the protective shielding effect resulted from an apolar or ordered microenvironment only could not increase the $S_1 \rightarrow T_1$ intersystem crossing efficiencies dramatically in this experiment. In the β-CD/TBZ/KI (Fig. 1a, $\lambda_{ex}/\lambda_{em} = 301/482$ nm or TX-100/TBZ/KI (Fig. 1b, $\lambda_{ex}/\lambda_{em} = 297/490$ nm) system, weak phosphorescence was observed, which suggested that although heavy-atom perturber KI could induce the $S_1 \rightarrow T_1$ intersystem crossing rates of TBZ to increase, ternary inclusion complex was not formed. In such a situation, the rigidity of the system was not strong enough to shield against light, oxygen and heat and the non-radiative decay of TBZ, such as the dissolved oxygen decay effect, collisions with solvent, conversion of energy, etc. deactivated its excited triple state and increased the $T_1 \rightarrow S_0$ non-radiative transition efficiencies. In the β-CD/TX-100/TBZ (Fig. 1c, $\lambda_{ex}/\lambda_{em} = 308/484$ nm) system, the weak phosphorescence observed indicated a novel and complex system formed among β-CD, TX-100, and TBZ, which strengthened the shielding effect and rigidity of the system, but lacked the induction effect of the heavy-atom perturber. Namely, the formation of a ternary inclusion complex was expected. For the β-CD/TX-100/TBZ/KI (Fig. 1e, $\lambda_{ex}/\lambda_{em} = 298/481$ nm) system, strong and reproducible phosphorescence was emitted, and the luminescence intensity increased greatly compared with that reported in reference [16] (Fig. 1d, $\lambda_{ex}/\lambda_{em} = 300/488$ nm), which indicated that the polarity and rigidity of the microenvironment around TBZ was decreased and increased, respectively. The obviously different phenomenon in the changes of phosphorescence intensity of TBZ in β-CD/TX-100/TBZ/KI system compared with other system provided more evidence to the formation of the ternary inclusion complex [21], which could do contributions to understand the interaction between TBZ and KI.

3.2. The supramolecular multirecognition interaction between β-CD, TX-100 and TBZ

3.2.1. Characterization of β-CD–TBZ inclusion complex

Formation of inclusion complex can be proved by IR spectrometry because the absorbance peaks of the included part of the guest molecule are generally shifted or their intensities altered [19]. By comparison of the enlarged IR spectra (in the regions of 600–1750 cm^{-1}) of TBZ (Fig. 2a), β-CD (Fig. 2b), the physical mixture of TBZ and β-CD (Fig. 2c) and the inclusion complex (Fig. 2d), it could be seen that the spectrum of c was essentially the combination of (a) and (b), which indicated that physical mixture cannot lead to inclusion; there were apparent differences between the spectra of (c) and (d) and some characteristic IR absorption peaks of TBZ and β-CD changed obviously in inclusion complex: the 1028–1151 cm^{-1} absorption band in inclusion complex assigned to the characteristic C–O–C bond antisymmetric stretching vibration and C–C/C–O bond stretching vibration of β-CD [22]; the 1300 cm^{-1} absorption peak (■), which could be assigned to the skeleton stretching vibration of heterocycle namely thiazole ring, appeared in inclusion complex; the 951 cm^{-1} absorption peak (⋆) due to the α-1,4 bond skeleton vibration of β-CD blue-shifted to 958 cm^{-1}; the benzene ring skeleton vibration absorption peak at 1580 cm^{-1} (●) of TBZ red-shifted to 1570 cm^{-1}; the 770 cm^{-1} (▼) absorption peak assigned to four adjoining hydrogens at benzene ring of TBZ blue-shifted to 776 cm^{-1}; the 1691 cm^{-1} (▲) 673 cm^{-1} (◣) absorption peaks of TBZ disappeared in inclusion complex.

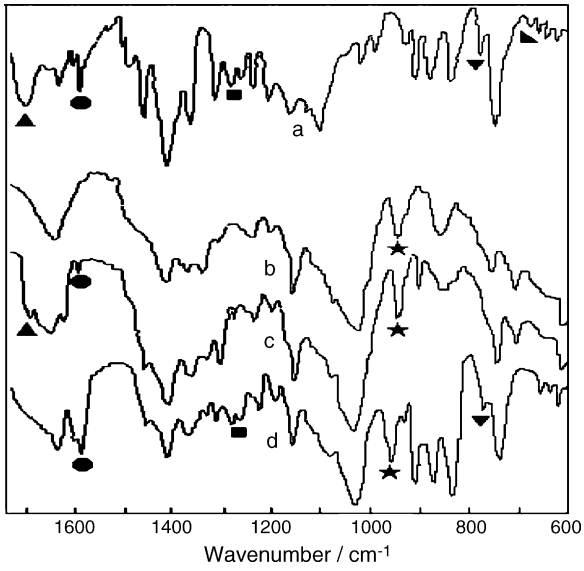

Fig. 2. The infra-red spectra of TBZ (a) β-CD (b), the physical mixture of TBZ and β-CD (c) and β-CD inclusion complex (d).

Table 1
Chemical shifts δ of protons in β-CD, TBZ and TBZ–β-CD inclusion complex

	β-CD						TBZ			
	H_1	H_2	H_3	H_4	H_5	H_6	H_1	H_2	H_3	H_4
$\delta_{\beta\text{-CD}}$ (δ_{TBZ})	4.83	3.28	3.64	3.34	3.59	3.64	7.25	7.60	8.52	9.36
$\delta_{\beta\text{-CD–TBZ}}$	4.80	3.26	3.54	3.33	3.50	3.56	7.18	7.53	8.51	9.35
[a]$\Delta\delta$	−0.03	−0.02	−0.10	−0.01	−0.09	−0.08	−0.07	−0.07	−0.01	−0.01

[a] $\Delta\delta = \delta_{\beta\text{-CD–TBZ}} - \delta_{\beta\text{-CD}}$ (δ_{TBZ}).

Based on these facts, it could be concluded preliminarily that the benzene ring of TBZ was included into the β-CD cavity to form a supramolecular inclusion complex.

According to the partial ^{1}H NMR spectra data of TBZ, β-CD and the inclusion complex, apparent changes in chemical shifts of different protons could be observed (Table 1): unlike the dramatical upfield shifts of β-CDs interior H-3, H-5 and H-6 protons, which resulted from the shielding effect exerted by the inclusion of TBZs benzene ring into β-CDs cavity, the shifts of β-CDs outside H-2 and H-4 protons could be neglected; the apparent shift changes of β-CDs H-3 indicated that the guest molecule entered β-CDs cavity along its wide rim which possessed secondary hydroxyls [23]; H-1 and H-2 of TBZs benzene ring protons had dramatical chemical shift changes and both upfielded 0.07 ppm, meanwhile other protons of TBZ changed little. All of the facts showed obviously that TBZs benzene ring was included into the β-CDs cavity, which was in good agreement with the results obtained from IR spectra.

3.2.2. Studies on the supramolecular interaction between β-CD and TX-100 by surface tension method

As shown in Fig. 3, in the absence of β-CD, the surface tension of the solutions began to decrease gradually with the increasing concentration of TX-100, the critical micelle concentration (CMC) was 0.22×10^{-3} mol/L. In the presence of β-CD, however, a continuous increase in β-CD concentration resulted in an increase in surface tension of the solutions. The addition of β-CD shifted the CMC* (apparent CMC) to higher concentrations (Table 2). This meant that the higher β-CD concentration was used, the higher TX-100 concentration was needed for the micelle formation. It also could be found that when the concentration of TX-100 was CMC*, the surface tension of the solutions was equal to that of the solutions that contained TX-100 in the concentration of CMC in the absence of β-CD, which indicated that β-CD or the inclusion complex formed between β-CD and surfactant was of no surface activity [24], and there was no interaction occurred between the inclusion complex and micelles because the micelles could not enter the β-CDs cavity which resulted from its disadvantageous structure. It was the surfactant monomers, not the micelles, contributed to the decreasing of the surface tension [25] and the formation of the inclusion complex. Variation in the surface tension of the solution and the CMC indicated the occurrence of supramolecular interaction between β-CD and TX-100 [26].

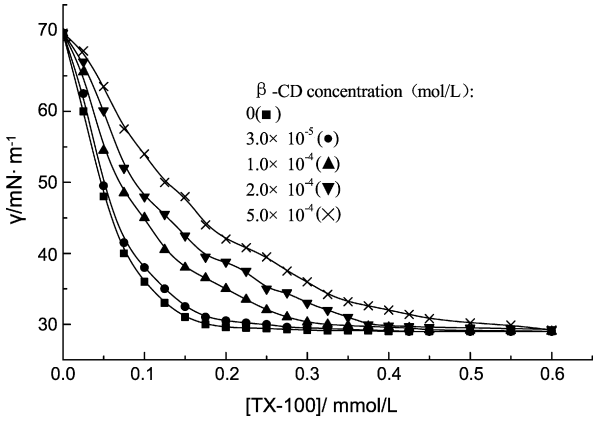

Fig. 3. Dependence of surface tension on surfactant concentrations at various concentrations of β-CD.

The stoichiometry of the β-CD:TX-100 system was determined by the equation below [13]:

$$\frac{1}{\Gamma_i} = \frac{1}{n} + \frac{1}{{}^0S_i} n K_A$$

where Γ_i was ${}^bS_i/C$, ${}^bS_i$ referred to the concentration difference values of TX-100 in the absence and presence of β-CD when the surface tension was fixed, C the concentration of β-CD added, ${}^0S_i$ the free concentration of TX-100 in the absence of β-CD, n the number of guest molecules included into the β-CDs cavity and K_A was the equilibrium constant. Fig. 4 showed a plot of $1/\Gamma_i$ versus $1/{}^0S_i$, it could be seen that there was a linear relationship between $1/\Gamma_i$ and $1/{}^0S_i$. The n could be got from the intercept and the K_A could be evaluated from the ratio of the intercept to slope, and the average values of K_A and n were listed in Table 2. According to the data the formation of a 1:1 β-CD:TX-100 inclusion complex was confirmed and the K_A was determined to be $(8.08 \pm 0.14) \times 10^3$ L/mol.

Table 2
CMC*, average equilibrium constant and inclusion ratio of TX-100 at different concentrations of β-CD

[β-CD] (mmol/L)	$CMC^*_{TX\text{-}100}$ (mmol/L)	K_A (L/mol)	n
0.03		$(9.11 \pm 0.12) \times 10^3$	0.94
0.10	0.31	$(8.56 \pm 0.13) \times 10^3$	1.13
0.20	0.40	$(7.52 \pm 0.21) \times 10^3$	1.15
0.30	0.46		
0.40	0.56		
0.50	0.59	$(7.13 \pm 0.10) \times 10^3$	1.12
0.60	0.59		
Average		$(8.08 \pm 0.22) \times 10^3$	1.08

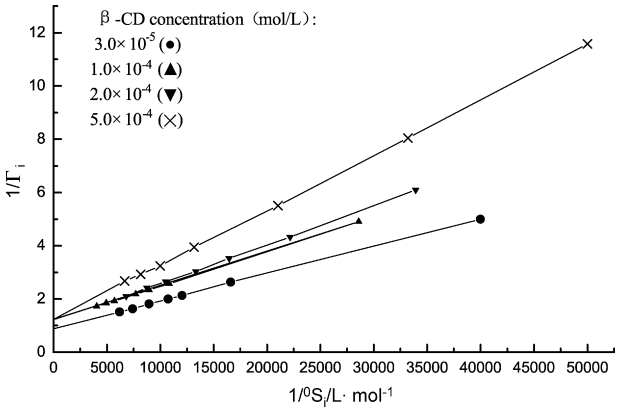

Fig. 4. $1/\Gamma_i$ plotted against $1/^0S_i$.

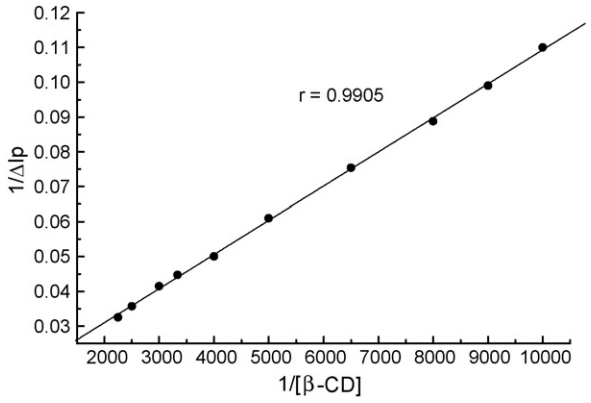

Fig. 6. Double reciprocal plot of the ternary inclusion complex.

3.2.3. Determination of apparent equilibrium constant of ternary inclusion complex

Equilibrium shifting method [27,28] was used to evaluate the stoichiometry of the β-CD:TBZ:TX-100 ternary complex. Keeping the concentration of TX-100 (Fig. 5a) and β-CD (Fig. 5b) at a constant value and plotting the logarithm of relative phosphorescence intensity against logarithm of concentration of beta-CD (Fig. 5a) and TX-100 (Fig. 5b) can give the stoichiometries of TBZ:β-CD and TBZ:TX-100, respectively. The slopes of the two plots were 1.14 and 1.10, respectively, suggesting the formation of a 1:1:1 ternary complex.

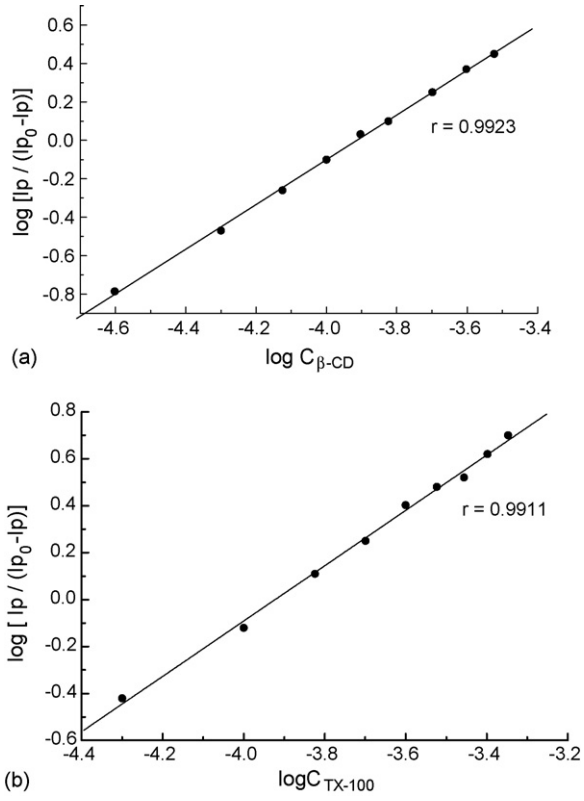

Fig. 5. Equilibrium shifting method for the determination of formation ratio of the ternary inclusion complex C_{TBZ} 200 μg/L; C_{KI} 0.20 mol/L; (a) $C_{TX\text{-}100}$ 4.0×10^{-4} mol/L; (b) $C_{\beta\text{-CD}}$ 5.0×10^{-4} mol/L.

The formation of the ternary inclusion complex could be described by following equation:

$$\text{TX-100} + \beta\text{-CD} + \text{TBZ} \overset{K}{\rightleftarrows} \text{TBZ} : \beta\text{-CD} : \text{TX-100}$$

The 1:1:1 stoichiometry of the β-CD:TBZ:TX-100 system was also confirmed by the Benesi–Hildebrand equation [29]:

$$\frac{1}{\Delta I_p} = \frac{1}{\alpha} K[\text{S}][\beta\text{-CD}] + \frac{1}{\alpha}$$

where K was the apparent equilibrium constant and ΔI_p was the difference in the phosphorescence intensity of TBZ in the presence and absence of β-CD. [S] and [β-CD] were the equilibrium concentration of TX-100 and β-CD, respectively. α was a combined instrumental constant. When the initial concentration of β-CD, $C_{\beta\text{-CD}}$, was much greater than that of the inclusion complex [β-CD] could be replaced by $C_{\beta\text{-CD}}$. The same principle can be applied to [S] when initial concentration of TX-100 was fixed at 6.0×10^{-4} mol/L and was used as the equilibrium concentration. Fig. 6 showed a representative double-reciprocal plot of $1/\Delta I_p$ versus 1/[β-CD] for the TBZ:β-CD:TX-100 system. As could be seen, a good linear relationship was observed with a correlation coefficient of 0.9905, which confirmed the 1:1:1 stoichiometry of a ternary inclusion complex in aqueous solution. The evaluated K from the ratio of the intercept to slope was $(3.42 \pm 0.23) \times 10^6$ L^2/mol^2.

3.2.4. Mechanism of the supramolecular multirecognition interaction

The process of the supramolecular multirecognition interaction was deduced and shown in Fig. 7: driven by the non-covalent force, such as the hydrophobic interaction, van der Waals force or hydrogen bonding force, TBZ, the first guest, entered β-CDs cavity along its wide rim which possessed secondary hydroxyls to form a 1:1 inclusion complex (Fig. 7I). When TX-100, the second guest, was added to the solution and driven by the non-covalent force, it reacted with β-CD by its hydrophobic moiety. But because of the spacial steric effect resulted from the occupation of β-CDs cavity space by TBZs phenyl ring and with its thiazole ring protruding from the cavity, not the whole hydrophobic part of TX-100, but its hydrocarbon chain could interact with β-CD and had no choice but to enter β-

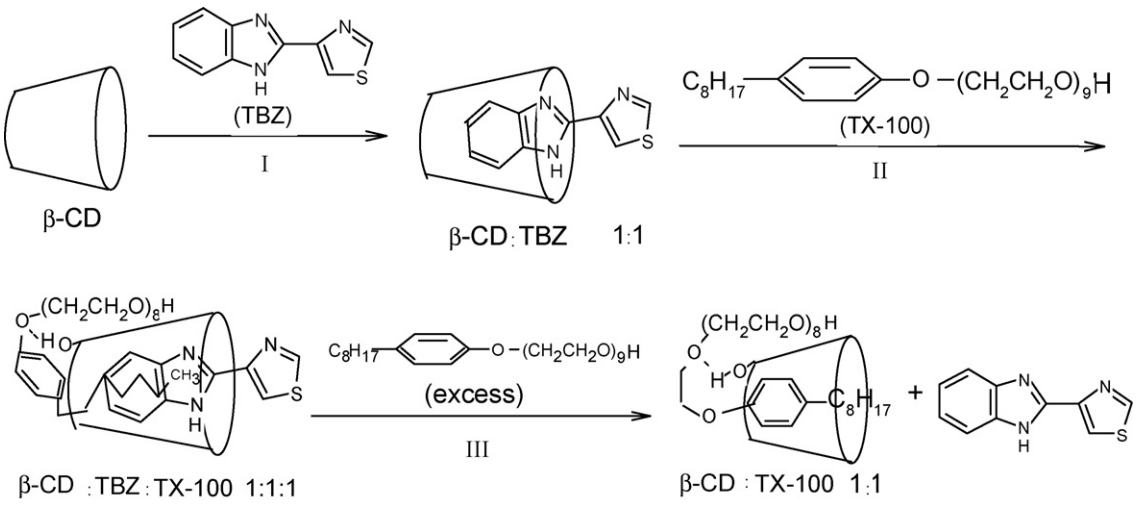

Fig. 7. The process of the supramolecular multirecognition interaction.

CDs cavity along its narrow rim to form a ternary inclusion complex of stoichiometry 1:1:1 (Fig. 7II). Other parts of TX-100 located outside the cavity, among which the phenyl ring covered at the narrow mouth of the cavity, the oxygen atom adjacent to the phenyl ring formed hydrogen bond with β-CDs primary hydroxyl to fix the complex, and the rest covered at the outside surface of β-CDs cavity that had more polarity, all of which provided a more hydrophobic microenvironment for TBZ to shield TBZ from oxygen and decrease the collision quenching of dissolved oxygen. The coiled hydrocarbon chain of TX-100 in β-CDs cavity not only expelled water molecules out of the cavity to decrease the quenching effect of dissolved oxygen, but acted as a wedge to limit the rotation of TBZ molecule and to offer a more rigidity microenvironment for TBZ to decrease the rates of non-radiative transition process of excited triplet state and increase the quantum yield of RTP. In conclusion, in the formation of the ternary inclusion complex, TX-100 acted as the spacial filler and regulator, as well as the hydrogen bond forming agent.

3.3. Effect of reaction conditions

3.3.1. Effect of pH

Fig. 8 showed the dependence of phosphorescence intensity on pH. It was not necessary to eliminate oxygen in this ternary system and the phosphorescence intensity present maximum and remained constant in the pH range of 2.5–11.5, which was greatly broadened compared with the method using chemical oxygen scavenger [16] (6.5–10). Sodium citrate–sodium hydroxide buffer solution was used to adjust pH to 5.50. When the pH was lower than 2.5, large quantities of onium salts were formed between TX-100 and protons [30], which increased the hydrophilic ability of TX-100 to increase the water quantity contained in the micellar interior layers, increased the quenching efficiencies of the dissolved oxygen. When the pH exceeded to 11.5, TBZ existed in the form of anion [31], which not only increased the hydrophilicity of the microenvironment, but increased the interaction distance between TBZ and I^- because of electrostatic repulsion, both resulting in decay of the phosphorescence.

3.3.2. Effect of KI concentration

The ether oxygen atoms of TX-100 had the similar interacting behavior to the oxygen atoms of crown ethers, which could coordinate with K^+ to make part of the micelle present positive electricity. Then I^- was enriched zonely by electrostatic attraction to decrease the distance between TBZ and I^-, and their interacting probabilities was increased drastically. Compared with the reported HAI-RTP method [16], the KI concentration was decreased dramatically to a concentration range of 0.15–0.45 and 0.20 mol/L was used. Since the heavy-atom perturber could increase the speed of $S_1 \rightarrow T_1$ intersystem transition and the speed of radiative transition of triplet state simultaneously to shorten the phosphorescence lifetime, evaluation of the phosphorescence lifetime of TBZ in the present experiment was carried out. According to the equation written as [32]: $\ln I_0 - \ln I_t = -t/\tau$, in the present experimental conditions, the

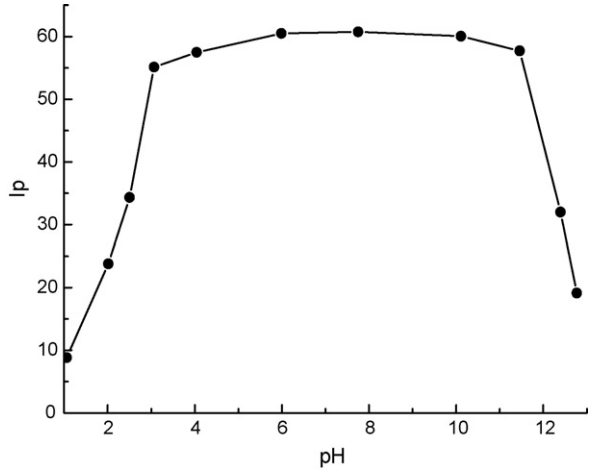

Fig. 8. Dependence of RTP on pH. C_{TBZ} 200 μg/L, C_{KI} 0.20 mol/L, $C_{\beta\text{-CD}}$ 5.0×10^{-4} mol/L and $C_{TX\text{-}100}$ 6.0×10^{-4} mol/L.

Table 3
Apparent formation constant (K), standard enthalpy (ΔH°), entropy (ΔS°) and free energy (ΔG°) changes of ternary inclusion complex as a function of temperature

Temperature (K)	298	303	308	313	318	323	328	333
$\ln K$	15.08	14.87	14.50	14.26	13.94	13.71	13.43	13.01
ΔG (kJ/mol)	−37.46	−37.29	−37.13	−36.96	−36.80	−36.63	−36.47	−36.29
ΔH (kJ/mol)				−47.29				
ΔS (kJ/mol)				−0.033				

average value of τ was determined from five measurements and was found to be 0.8 ms, that was increased nine times compared with that reported in reference [16].

3.3.3. Effect of β-CD concentration

A study on the dependence of RTP on the β-CD concentration was performed. In the concentration range of 3.0×10^{-4} to $\sim 8.0 \times 10^{-4}$ mol/L, RTP was the highest and remained constant. In the experiment, 5.0×10^{-4} mol/L β-CD was used.

3.3.4. Effect of TX-100 concentration

The influence of TX-100 concentration was studied. It could be observed that in the TX-100 concentration range of 6.0×10^{-4} to $\sim 6.3 \times 10^{-4}$ mol/L, RTP was the highest and remained constant, when exceeded 6.3×10^{-4} mol/L, RTP began to gradually decrease, then 6.0×10^{-4} mol/L TX-100 was fixed. It was found that the optimum concentration of TX-100 (6.0×10^{-4} mol/L) was a bit higher than the CMC* (5.9×10^{-4} mol/L, Table 2) in the presence of 5.0×10^{-4} mol/L β-CD, which indicated that there was two forms of TX-100 coexisted in the solution: monomers and micelles. The monomers acted as the spacial filler and regulator, as well as the hydrogen bond forming agent in the formation of the ternary inclusion complex. The micelles aggregated around the inclusion complex to provide a more hydrophobic microenvironment for the complex through its hydrophobic interior layers. When the TX-100 concentration was higher than a certain value (6.3×10^{-4} mol/L in this reaction condition), more and more TX-100 molecules were driven by the hydrophobic force to compete with TBZ for β-CDs cavity. The final results were that the TBZ molecules were expelled from β-CDs cavity and were dissolved in a mixed solution with great deal of micelles and β-CD, which was extremely different from the microenvironment experienced in the ternary inclusion complex. When the shielding protection for the triplet state of TBZ was removed, the intermolecular collision was reinforced, and the rate of non-radiative decay process was increased, which led to the phosphorescence quantum yield drastically decreased and phosphorescence quenching occurred.

3.4. Inclusion complex thermodynamics

Along with the increasing of system temperature, intermolecular collision was reinforced to make the supramolecular multi-recognition interaction weaken, which made the inclusion complex gradually dissociate and the phosphorescence decrease. But the fact that TBZ still showed relatively intense phosphorescence at 55 °C reflected that the ternary inclusion complex was rather stable.

The thermodynamics parameters, standard free energy (ΔG°), enthalpy (ΔH°) and entropy (ΔS°) for the inclusion complexes were obtained from the van't Hoff equation: $\ln K = -\Delta H^\circ/RT + \Delta S^\circ/\mathrm{R}$. The ΔH° and ΔS° of the complex formation were calculated from the slope and intercept by plotting $\ln K$ versus $1/T$ and ΔG° was obtained according to the equation $\Delta G^\circ = \Delta H^\circ - T\Delta S^\circ$. The calculated results were shown in Table 3. As could be seen, the ΔH°, ΔG°, and ΔS° were all negative, indicating that the complex process was spontaneous, thermodynamics stable, enthalpy-driven, and not entropy-driven. The positive entropy variation resulted from the hydrophobic interaction was smaller than the negative enthalpy and entropy variation resulted from Van der Waals force and hydrogen bonding of the complex process [22]. Temperature increase did not show favorites to the process because of its heat release character.

4. Conclusions

A strong and reproducible room temperature phosphorescence signal come from a 1:1:1 β-cyclodextrin/thiabendazole/Triton X-100 supramolecular ternary inclusion complex could be induced by KI as a heavy-atom perturber without removing dissolved oxygen from solution. TX-100 was proved to play an important role in the formation of the inclusion complex, which can be concluded as follows: (1) TX-100 had spacial fill and regulation effect on the ternary inclusion complex because the TX-100 alkyl chains can wedge into the cavity of β-CDs cavity to offer a more rigidity microenvironment for TBZ, which dramatically decreased the rates of the $T_1 \rightarrow S_0$ radiationless transition decay process; (2) the phenyl ring of TX-100 acted as a lid for the cavity of β-CD by cup hydrogen bond formation between the ether oxygen atoms of TX-100 and the primary hydroxyls of β-CD, Moreover, in the hydrophobic cavity of β-CD, TBZ can be soluble in the micellar interior layers, which effectively shielded TBZ from oxygen and decreased the collision quenching of dissolved oxygen; (3) the ether oxygen atoms of TX-100 coordinated with K^+, which made the distance between K^+–TBZ and I^- decrease under the function of electrostatic attraction and caused their interaction increase. Therefore the $T_1 \rightarrow S_1$ radiationless transition decrease dramatically. The formation of the inclusion complex protected the phosphorescence against varying quenching factors, drastically decreased the concentration of heavy-atom perturber and optimized experimental conditions.

Acknowledgements

This work was supported by Program for New Century Excellent Talents in University (NCET-04-0651), the National Natural Science Foundation of China (nos. 20335030 and 20575036).

References

[1] W. Saenger, Angew. Chem. Int. Ed. 19 (1980) 344.
[2] G. Wenz, Angew. Chem. Int. Ed. 33 (1994) 803.
[3] J. Szejtli, Chem. Rev. 98 (1998) 1743.
[4] Y. Takakura, M. Hashida, Pharm. Res. 13 (1996) 820.
[5] B. Pfannemuller, W. Burchard, Makromol. Chem. 121 (1969) 1.
[6] S. Li, W.C. Purdy, Chem. Rev. 92 (1992) 1457.
[7] R. Breslow, A.D. Dong, Chem. Rev. 98 (1998) 1997.
[8] A. Ueno, T. Kuwabara, A. Nakamura, F. Toda, Nature 356 (1992) 136.
[9] A. Ueno, Supramol. Sci. 3 (1996) 31.
[10] H. Ye, W. Tong, V.T. D'Souza, J. Am. Chem. Soc. 114 (1992) 5470.
[11] S.R. Mcalpine, M.A. Garcia-Garibay, J. Am. Chem. Soc. 120 (1998) 4269.
[12] M. Lahav, K.T. Ranjit, E. Katz, I. Willner, Chem. Commun. (1997) 259.
[13] I.M. Klotz, F.M. Walker, R.B. Pivan, J. Am. Chem. Soc. 68 (1946) 1486.
[14] A.E. Kaifer, Adv. Supramol. Chem. 2 (1992) 1.
[15] M.D. Veiga, F. Ahsan, Eur. J. Pharm. Sci. 9 (2000) 291.
[16] A. Segura-Carretero, C. Cruces-Blanco, B. Cañabate-Díaz, J.F. Fernández-Sánchez, A. Fernández-Gutiérrez, Anal. Chim. Acta 417 (2000) 19.
[17] L.D. Li, X.K. Chen, L. Mou, W.Q. Long, A.J. Tong, Anal. Chim. Acta 424 (2000) 177.
[18] Y.Z. Hui, J.H. Gu, Acta Chim. Sinica 39 (1981) 309.
[19] L. Szente, Comprehensive of Supramolecular Chemistry, in: J.L. Atwood, J.-M. Lehn (Eds.), Cyclodextrins, vol. 3, Pergamon, Oxford, U.K., 1996 (Chapter 7).
[20] Z.K. Zhou, T.R. Gu, J.M. Ma, Base of Colloid Chemistry, 2nd ed., Beijing University Press, Beijing, 1996, p. 26.
[21] X.Z. Du, Y. Zhang, Y.B. Jiang, L. Lin, X.Z. Huang, G.Z. Chen, Acta Chim. Sinica 56 (1998) 453.
[22] L.H. Tong, Chemistry of Cyclodextrin-Foundation and Application, 1st ed., Science Press, Beijing, 2001.
[23] V. Rudiger, A. Eliseev, S. Simova, H.J. Schneider, M.J. Blandamer, P.M. Cullis, A.J. Meyer, J. Chem. Soc., Perkin Trans. 2 (1996) 2119.
[24] U.R. Dharmawardana, S.D. Christian, E.E. Tucker, R.W. Taylor, J.F. Scamehorn, Langmuir 9 (1993) 2258.
[25] N. Funasaki, Bull. Chem. Soc. Jpn. 65 (1992) 1323.
[26] J. Idem, Collid. Inter. Sci. 79 (1981) 313.
[27] H.E. Bent, C.L. French, J. Am. Chem. Soc. 63 (1941) 568.
[28] F. Capitán, A.A. Ramirez, C.J. Linares, Analyst 111 (1986) 739.
[29] S. Hamai, J. Am. Chem. Soc. 111 (1989) 3954.
[30] P. Becher, J. Collid. Sci. 17 (1962) 801.
[31] C.T. Patricia, L.C. Love, J. Phys. Chem. 86 (1982) 5227.
[32] G.G. Giachino, J. Chem. Phys. 52 (1970) 2964.